Electronic Supplementary Information

Hydrophobic Surface Enabled Salt-blocking 2D Ti_3C_2 MXene Membrane for Efficient and Stable Solar Desalination

Jianqiu Zhao†, Yawei Yang†, Chenhui Yang, Yapeng Tian, Yan Han, Jie Liu, Xingtian Yin, and Wenxiu Que*

Electronic Materials Research Laboratory, Key Laboratory of the Ministry of Education, International Center for Dielectric Research, and Shaanxi Engineering Research Center of Advanced Energy Materials and Devices, School of Electronic & Information Engineering, Xi'an Jiaotong University, Xi'an 710049, P. R. China

∗ Corresponding author:
Tel.: +86-29-83395679; Fax: +86-29-83395679
Email address: wxque@mail.xjtu.edu.cn (W. X. Que)
† These authors contributed equally to this work

Lists of Content

Synthesis of Ti_3AlC_2 powder

The MAX phase was used as precursor for MXene synthesis. Ti_3AlC_2 was prepared by vacuum atmosphere sintering method through mixing all powders of TiC (2-4 μm particle size, 99% purity, Aladdin), Al (1-3 μm particle size, 99.5% purity, Aladdin), and Ti (≤ 48 μm particle size, 99.99% purity, Aladdin) in a molar ratio of 2:1.2:1. The mixed powders were ball-milled with ethyl alcohol for 4 h at a speed of 300 rpm, and dried in the vacuum oven at 60 °C for 24 h. Then, the mixture was annealed in an alundum tube in Ar gas at a flow of 100 mL min^{-1}. Sintering process was conducted at 1400 °C for 2 h at a heating rate of 8 °C min^{-1}. The sintered product was grinded by stainless steel mortar and sieved through a 400 mesh screen, so that the initial particle size was controlled < 38 μm. Thus, the Ti_3AlC_2 powders were obtained for further use.

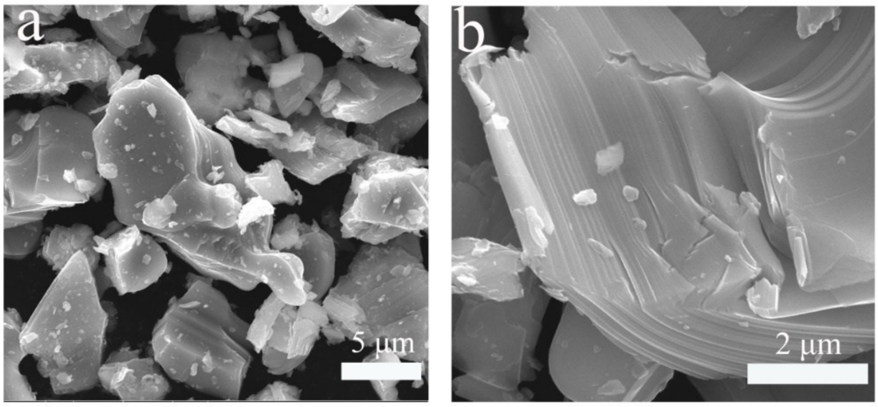

Fig. S1 SEM images of the Ti_3AlC_2 powder.

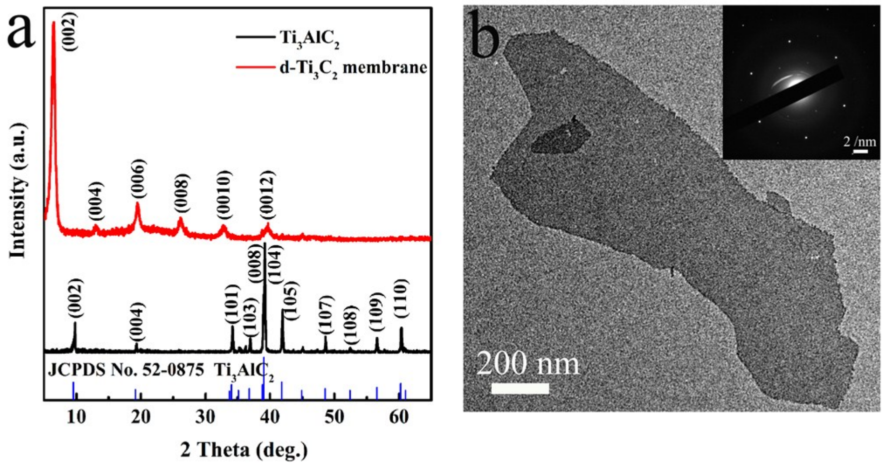

Fig. S2 (a) XRD patterns of Ti_3AlC_2 and d-Ti_3C_2. (b) TEM image of a d-Ti_3C_2 nanosheet (inset: SAED pattern).

Characterizations of Ti_3AlC_2 and d-Ti_3C_2 sample

Fig. S1 shows the SEM images of the Ti_3AlC_2 powders, which serves as raw layered materials for the d-Ti_3C_2 nanosheets preparation by selectively etching their Al layers. Fig. S2a is the XRD patterns of the as-prepared Ti_3AlC_2 and d-Ti_3C_2. It can be noted that the raw diffraction peaks are matched well with the Ti_3AlC_2 MAX standard pattern (JCPDS No. 52-0875). After being etching by HCl/LiF and sonication treatment of MAX powders, the typical diffraction peak (002) of Ti_3C_2 shifts to a much lower angle, resulting from an increased c lattice parameter. Fig. S2b presents the TEM image of an individual d-Ti_3C_2 nanosheet, showing its ultrathin 2D nanosheet morphology with lateral sizes up to a few hundred nanometers. The selected area electron diffraction (SAED) pattern as seen in the inset of Fig. S2b verifies the crystalline and hexagonal symmetry of d-Ti_3C_2 again.

Table S1 Solar evaporation performance based on hydrophobic d-Ti_3C_2 MXene membrane in this work compared with other membrane materials under one sun.

Sample	Hydropathy	Evaporation rate (kg/m^2 h)	Efficiency (%)	Desalination application	Salt-blocking solution	Reference
Carbon based DLS	Hydrophilic	1.2	64	No	-	1
Au NP/NPT	Hydrophilic	~1	~64	No	-	2
Ti_2O_3 NP	Hydrophilic	1.32	-	No	-	3
Functionalized Graphene	Hydrophilic	0.47	48	No	-	4
rGO/PU	Hydrophilic	0.9	65	No	-	5
Carbonized Mushroom	Hydrophilic	1.475	78	No	-	6
Artificial tree	Hydrophilic	1.08	74	No	-	7
TiAlON/NiO	Hydrophilic	1.13	73	No	-	8
Wood/CNT	Hydrophilic	0.95	65	No	-	9
Al NP/AAM	Hydrophilic	1	58	Yes	No	10
GO with 2D water path	Hydrophilic	1.45	80	Yes	No	11
Plasmonic wood	Hydrophilic	~1.0	~67	Yes	Microchannels	12
Tree-inspired design	Hydrophilic	~0.8	57.3	Yes	Microchannels	13
SWCNT/MoS_2	Hydrophilic	~1.1	81	Yes	No	14
Porous N-doped graphene	Hydrophilic	1.5	80	No	-	15
PPy-coated SS mesh	Hydrophobic	0.92	58	No	-	16
Ti_3C_2 MXene	Hydrophilic	1.33	84	No	-	17
Ti_3C_2 MXene	**Hydrophobic**	**1.31**	**71**	**Yes**	**Hydrophobic surface**	**This work**

References

1. H. Ghasemi, G. Ni, A. M. Marconnet, J. Loomis, S. Yerci, N. Miljkovic and G. Chen, *Nat. Commun.*, 2014, **5**, 4449.
2. L. Zhou, Y. Tan, D. Ji, B. Zhu, P. Zhang, J. Xu, Q. Gan, Z. Yu and J. Zhu, *Sci. Adv.*, 2016, **2**, e1501227.
3. J. Wang, Y. Li, L. Deng, N. Wei, Y. Weng, S. Dong, D. Qi, J. Qiu, X. Chen and T. Wu, *Adv. Mater.*, 2017, **29**, 1603730.
4. J. Yang, Y. Pang, W. Huang, S. K. Shaw, J. Schiffbauer, M. A. Pillers, X. Mu, S. Luo, T. Zhang, Y. Huang, G. Li, S. Ptasinska, M. Lieberman and T. Luo, *ACS Nano*, 2017, **11**, 5510-5518.
5. G. Wang, Y. Fu, A. Guo, T. Mei, J. Wang, J. Li and X. Wang, *Chem. Mater.*, 2017, **29**, 5629-5635.
6. N. Xu, X. Hu, W. Xu, X. Li, L. Zhou, S. Zhu and J. Zhu, *Adv. Mater.*, 2017, **29**, 1606762.
7. H. Liu, C. Chen, G. Chen, Y. Kuang, X. Zhao, J. Song, C. Jia, X. Xu, E.; Hitz, H. Xie, S. Wang, F. Jiang, T. Li, Y. Li, A. Gong, R. Yang, S. Das and L. Hu, *Adv. Energy Mater.*, 2017, 1701616.
8. H. Liu, X. Zhang, Z. Hong, Z. Pu, Q. Yao, J. Shi, G. Yang, B. Mi, B. Yang, X. Liu, H. Jiang and X. Hu, *Nano Energy*, 2017, **42**, 115-121.
9. C. Chen, Y. Li, J. Song, Z. Yang, Y. Kuang, E. Hitz, C. Jia, A. Gong, F. Jiang, J. Y. Zhu, B. Yang, J. Xie and L. Hu, *Adv. Mater.* 2017, **29**, 1701756.
10. L. Zhou, Y. Tan, J. Wang, W. Xu, Y. Yuan, W. Cai, S. Zhu and J. Zhu, *Nat. Photon.*, 2016, **10**, 393-398.
11. X. Li, W. Xu, M. Tang, L. Zhou, B. Zhu, S. Zhu and J. Zhu, *Proc. Natl. Acad. Sci.*, 2016, **113**, 13953-13958.
12. M. Zhu, Y. Li, F. Chen, X. Zhu, J. Dai, Y. Li, Z. Yang, X. Yan, J. Song, Y. Wang, E. Hitz, W. Luo, M. Lu, B. Yang and L. Hu, *Adv. Energy Mater.*, 2017, 1701028.
13. M. Zhu, Y. Li, G. Chen, F. Jiang, Z. Yang, X. Luo, Y. Wang, S. D. Lacey, J. Dai, C. Wang, C. Jia, J. Wan, Y. Yao, A. Gong, B. Yang, Z. Yu, S. Das and L. Hu, *Adv. Mater.*, 2017, **29**, 1704107.
14. X. Yang, Y. Yang, L. Fu, M. Zou, Z. Li, A. Cao and Q. Yuan, *Adv. Funct. Mater.*, 2017, 1704505.
15. Y. Ito, Y. Tanabe, J. Han, T. Fujita, K. Tanigaki and M. Chen, *Adv. Mater.*, 2015, **27**, 4302-4307.
16. L. Zhang, B. Tang, J. Wu, R. Li and P. Wang, *Adv. Mater.*, 2015,**27**, 4889-4894.
17. R. Li, L. Zhang, L. Shi and P. Wang, *ACS Nano*, 2017, **11**, 3752-3759.

Table S2 Structural parameters of the samples according to the (002) XRD peak.

Sample	2θ (degree)	*d* spacing (nm)
Hydrophilic d-Ti_3C_2 membrane	6.440	1.371
Hydrophobic d-Ti_3C_2 membrane	5.860	1.507

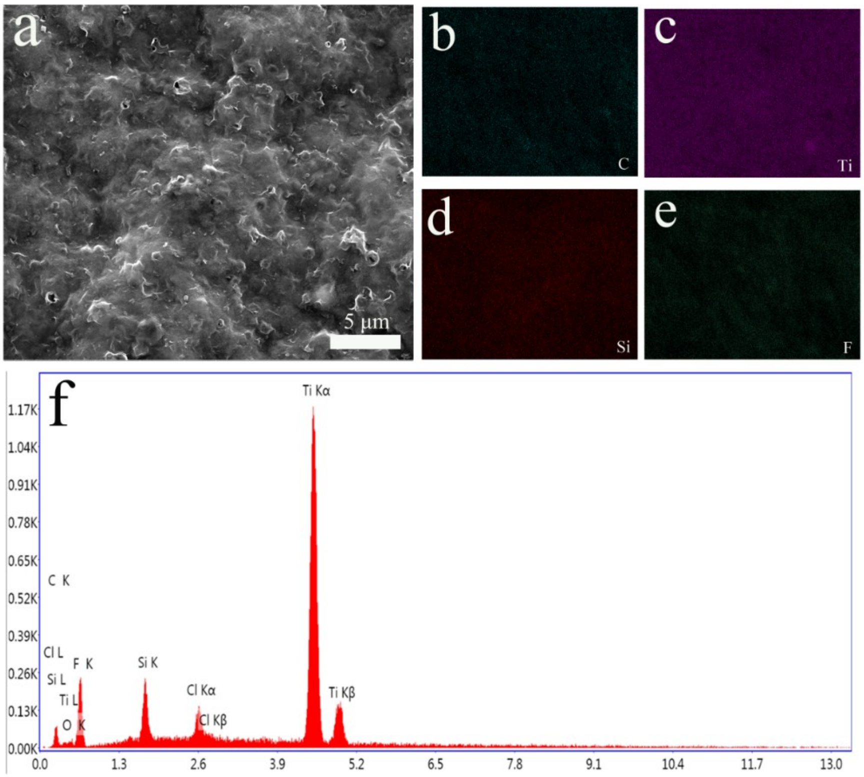

Fig. S3 (a) SEM image and corresponding (b-e) EDS mappings and (f) EDS spectrum of the hydrophobic d-Ti_3C_2 membrane.

Table S3 Solar evaporation performance of the hydrophilic and hydrophobic d-Ti_3C_2 membranes.

Mass loading (mg)		2	4	8	10
Hydrophilic membrane	Evaporation rate (kg/m^2 h)	1.28	1.32	1.36	1.41
	Receiver efficiency (%)	66	68	71	74
Hydrophobic membrane	Evaporation rate (kg/m^2 h)	1.17	1.20	1.24	1.31
	Receiver efficiency (%)	61	63	66	71

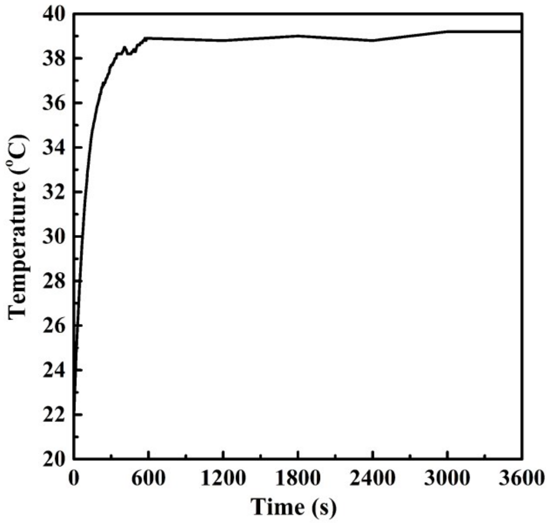

Fig. S4 Vapor temperature on the membrane surface during solar steam generation.

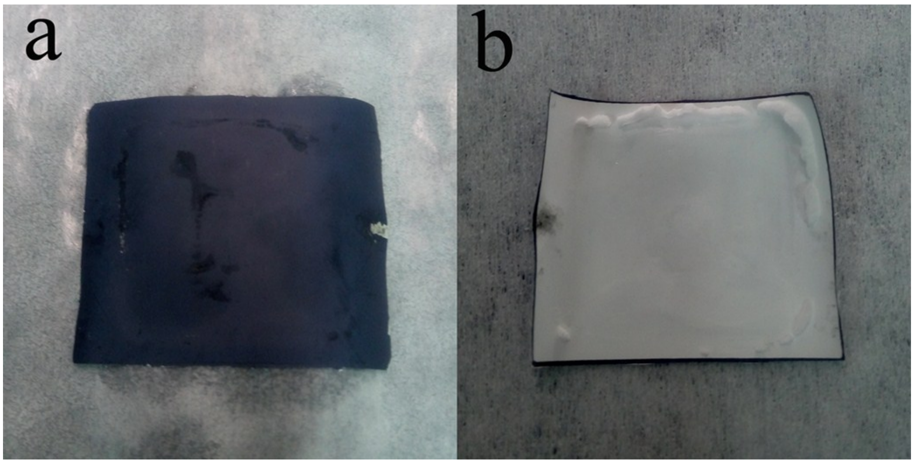

Fig. S5 Optical photographs of the (a) front and (b) back sides of the hydrophobic d-Ti_3C_2 membrane after 200 h solar desalination.

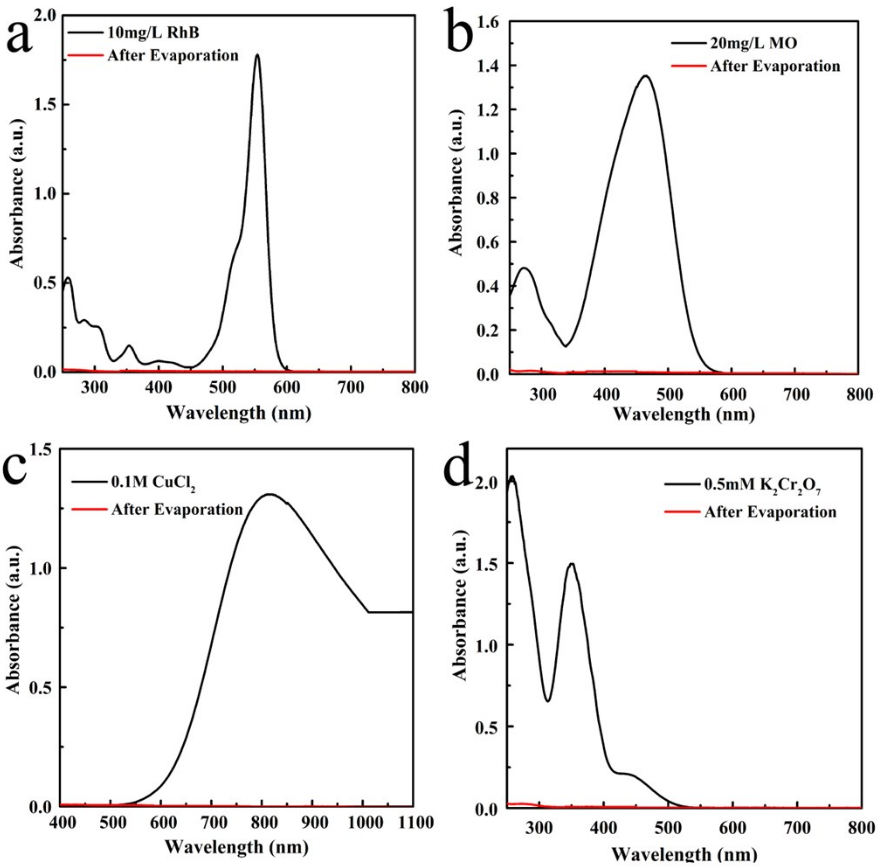

Fig. S6 UV-Vis spectra of organic dyes (a) RhB and (b) MO, and heavy metal ions (c) Cu^{2+} and (d) Cr^{6+} aqueous solution before and after evaporation purification.

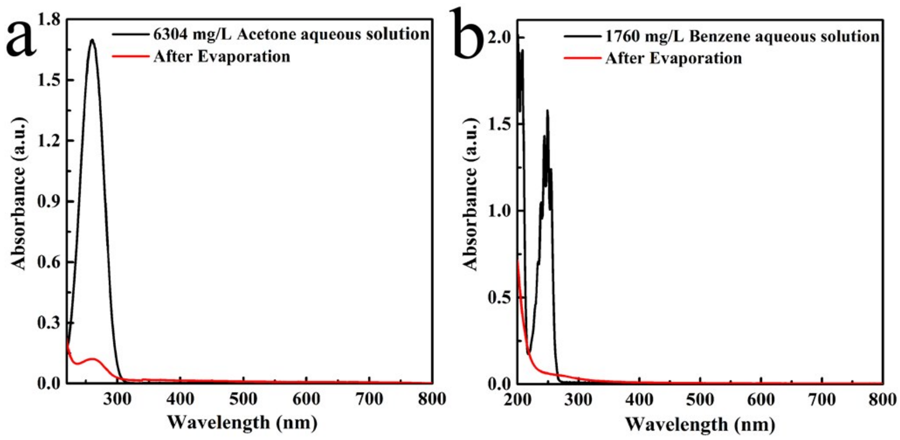

Fig. S7 UV-Vis spectra of volatile organics (a) acetone and (b) benzene aqueous solution before and after evaporation purification.